SAND2007-5343C

ELECTRO-THERMAL SIMULATION STUDIES FOR PULSED VOLTAGE FAILURES IN MICROSTRUCTURED ZNO VARISTORS

G. Zhao, R. P. Joshi[a]
Department of Electrical & Computer Engineering
Old Dominion University, Norfolk, VA 23529, USA.

H. P. Hjalmarson
Sandia National Laboratories, Albuquerque, NM 87185, USA.

Abstract

Time-dependent, two-dimensional simulations based on random Voronoi networks have been developed to study the internal heating and related breakdown effects in ZnO varistors in response to high-voltage pulsing. The focus is on internal grain-size variations and relative disorder. Our results predict that parameters such as the device hold-off voltage, the average internal temperature, and average dissipated energy density would be higher with more uniform grains. This uniformity is also predicted to produce lower thermal stresses and to allow for the application of longer duration pulses. Finally, it is shown that the principle failure mechanism arises from internal localized melting, while thermal stresses are well below the thresholds for cracking.

I. INTRODUCTION

Zinc oxide varistors are ceramic devices made by sintering ZnO powder together with small amounts of other oxide additives such as Bi_2O_3, MnO_2, Co_3O_4 etc. The resulting structure is granular, with a distribution of internal grain sizes. The presence of Bi-ions trapped at the grain-boundaries (GBs) is thought to be responsible for a highly nonlinear current–voltage (*I–V*) characteristics. Empirically $I \sim V^a$, where *a* can be 50 or higher, and these devices are ideally suited for use in electrical surge arresters [1-4].

In the micro-structured ZnO devices, energy states are created due to dislocations and dangling bonds arising from the crystallographic mismatch between adjacent grains. Free carriers (usually electrons present in the slightly n-type ZnO material) are trapped, leading to the creation of electro-static barriers at the interface. The potential barrier prevents current conduction, and offers the large impedance at relatively low voltages and non-linear *I-V* characteristics.

It is also known that not all grain boundaries exhibit non-linear electrical properties. A mixture of "good" (i.e. highly non-linear double Schottky junctions), "bad" (i.e. junction with poor non-linearity) and Ohmic grain boundaries are typically representative [5-8] of samples.

In this contribution, we focus on both the grain size non-uniformity and relative disorder within the ZnO, and investigate their influence on the electrical response and possible breakdown from high voltage pulsing. A physically based numerical model is developed to represent the random granular structure with its individual grain-boundaries. Variability in GB electrical behavior is accounted by incorporating a Gaussian distribution of non-linear I-V characteristics. For self-consistency, a coupled electro-thermal analysis, previously reported by our group [9], is used to determine the voltage driven temperature increases and possible material failure in a ZnO varistor.

II. MODELING DETAILS

A. Microstructure model for ZnO varistor

In order to include the stochastic granular aspects, the polycrystalline material has been modeled in terms of a random, two-dimensional, Voronoi [10] network. As an example in Fig. 1, a total of 986 grains have been used. The Voronoi structure is set up by generating N random seeds that correspond to N locations (x_i, y_i) within the entire simulation region. The polygons are then formed by the intersection of perpendicular bisectors from lines that connect neighboring seeds.

While the above includes granularity, variations in the internal disorder can be represented by appropriately controlling the positions of the N random seeds. The position of these seeds can be allowed to deviate by a displacement vector determined by two parameters: (i) the disorder length d (d>0) and, (ii) an angle θ ($0 \le \theta \le 2\pi$). The radius and angle of the displacement vector are uniformly distributed within the intervals [0, $d \times s$] and [0,2π], respectively. Fig. 2 shows the Voronoi networks with different values of the disorder parameter d. For very small values of d (e.g., d=0), a completely ordered honey-comb pattern results.

[a] Electronic mail: rjoshi@odu.edu

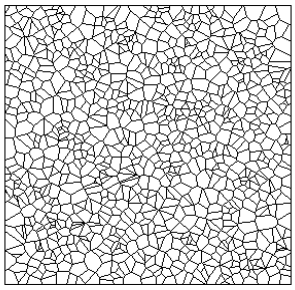

Figure 1. Voronoi network containing 986 cells.

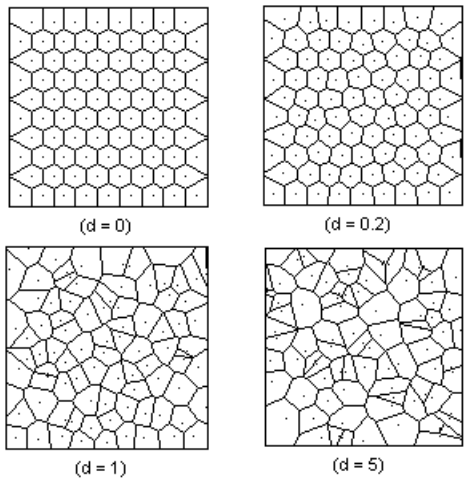

Figure 2. Voronoi networks with different disorder lengths "d."

B. Currents and Joule heating in ZnO varistors

In ZnO varistors, the dominant resistance arises from the GB, while each grain has a significantly lower resistance by comparison. Hence, only the non-linear current-voltage characteristics of each GB were considered. In particular, the following J-V characteristics (after [11]) were used to model each GB:

$$J_{ij}(U_{ij})=\begin{cases}\dfrac{A_1}{\rho_{gb}}\exp\left[-\dfrac{E_g-\beta\sqrt{|U_{ij}|}}{K_bT}\right]+A_2\left[\dfrac{|U_{ij}|}{V_B}\right]^{\alpha}; & |U_{ij}|\le V_U\\ \dfrac{A_1}{\rho_{gb}}\exp\left[-\dfrac{E_g-\beta\sqrt{V_U}}{K_bT}\right]+A_2\left[\dfrac{V_U}{V_B}\right]^{\alpha}+\dfrac{\left[|U_{ij}|-V_U\right]}{d_{ij}\rho_g}, & |U_{ij}|>V_U\end{cases} \quad , \quad (1)$$

where J_{ij} denotes the current density flowing through the GB between grains *i* and *j* in *A/cm*^{2}, and $U_{ij}=(U_i-U_j)$, with U_i and U_j being the voltages across grains *i* and *j*, and *T* the grain boundary temperature in Kelvin. Also in (1), V_B is the barrier voltage taken to be non-uniform, random variable for each grain boundary chosen from a normal distribution function $p(V_B)$ given by:

$$p(V_B)=\frac{1}{\sqrt{2\pi}\times 0.2}\exp\left[\frac{(V_B-3.2)^2}{2\times 0.2^2}\right], \quad V_B>0. \quad (2a)$$

The parameter α denotes a nonlinear coefficient and also follows a normal distribution $p(\alpha)$:

$$p(\alpha)=\frac{1}{\sqrt{2\pi}\times 50}\exp\left[\frac{(\alpha-7)^2}{2\times 50^2}\right], \quad \alpha>1. \quad (2b)$$

Finally, V_U is the critical upturn voltage in the high electrical field region, $V_U=V_B\left(J_U/A_2\right)^{1/\alpha}$, where J_U is the critical upturn current in high electrical field region [11]. Here J_U was chosen to be 10^3 A/cm^2 as reported elsewhere [11]. The other parameters in (1) are listed in Table 1.

Table 1. The various parameters of Eq. (1).

Symbol	Meaning	Unit	Value
A_1	constant	$A\cdot\Omega/cm$	2.5×10^{16}
A_2	constant	$A\cdot\Omega/cm^2$	0.01
ρ_{gb}	resistivity of grain boundary	$\Omega\cdot cm$	10^{12}
ρ_g	resistivity of grain	$\Omega\cdot cm$	1
E_g	barrier height	eV	0.8
β	constant	$eV^{1/2}$	2.83×10^{-2}
K_b	Boltzmann's constant	eV/K	8.625×10^{-5}

The above formulation allows for stochastic variations via the barrier voltage V_B. For example, we adopt a mean barrier voltage of 3.2 V with different variances. The external, electrical voltage was applied between the top and bottom edges of the Voronoi network. The nodal voltage equations were derived from the branched circuit schematic shown in Fig. 3 by applying the Kirchhoff current law at the ith node of an N-node circuit. The solution then yields currents flowing through the GBs as calculated by (1). The Joule heat generated at each GB is given as: $P_{ij}=sl_{ij}V_{ij}J_{ij}$, where V_{ij} and J_{ij} denote the voltage difference and current density between adjacent granular regions, and l_{ij} is the length of their common GB, and *s* is the thickness of the sample. Here, *s* is assumed to equal the average size of the grains.

C. Heat transfer and thermal stress calculations

It is assumed that the average temperatures of cells *i* and *j* are T_i and T_j, and that their initial values are at the ambient temperature (300K in this paper). The heat (dQ_i) transferred into cell *i* during time duration *dt* is approximately determined by:

$$dQ_i=\sum_j dQ_{ij}=\sum_j\left(T_i-T_j\right)\frac{sl_{ij}}{d_{ij}}k_T dt \quad (J) \quad , \quad (3)$$

where l_{ij} is the length of the common side between adjacent grains, d_{ij} is the distance between the centers of the two adjacent grains, T_j the average temperature of the adjacent grain j, and k_T the thermal conductivity of ZnO varistors taken to be: $k_T = 5.7\times10^{-2} W\cdot cm^{-1}\cdot K^{-1}$.

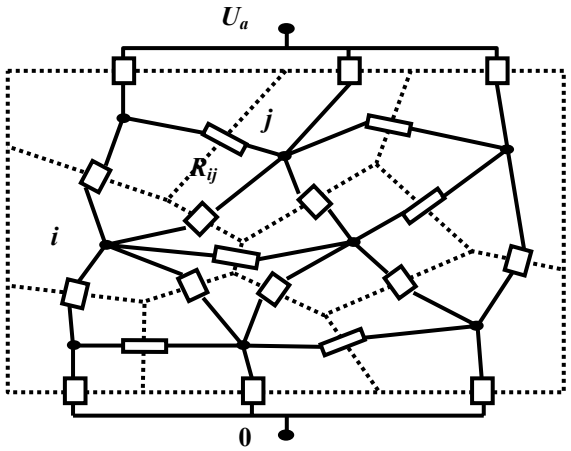

Figure 3. Conceptual circuit for the microscopic simulation of a ZnO varistor.

The temperature rise dT_i of grain i during dt is then given by the following equation:

$$dT_i = \frac{P_i dt + dQ_i}{S_i s \rho C_p} \quad (K) \quad , \tag{4}$$

where S_i denotes the area of the grain i, the ZnO varistor film thickness s is the average grain size, ρ = 5.6 g/cm^3 is the mass density of ZnO, $P_i = 0.5P_{ij}$, and C_p is the thermal capacity of ZnO ceramics taken to be:

$$C_p = 0.498\left[1+0.000828\left(T_i-20\right)\right] J/\left(g\cdot K\right) . \tag{5}$$

If the temperatures between two adjacent grains (say i and j) are unequal, then a thermal stress f_{ij} develops between them [12]. The expression for f_{ij} is given by:

$$f_{ij} = \frac{Ea\left(T_i - T_j\right)}{1-\mu} \quad \left(MPa\right) \quad , \tag{6}$$

where E is the Young's modulus taken to be 6.9×10^4 MPa, μ is the Poisson ratio equal to 0.3, and α is the linear expansion coefficient of ZnO varistor ceramics of about $4.86\times10^{-6} K^{-1}$ [11].

With large current flowing through ZnO varistors, the localized temperature at grain boundaries can dramatically increase and even exceed the 820˚C melting point of Bi_2O_3 in the GB [11]. Upon melting as the barrier in the GB vanishes, the conductivity is assumed to then switch over to an Ohmic, highly resistive characteristic:

$$J = V/(2\times10^7) \quad \left(A/cm^2\right) \quad . \tag{7}$$

Though other I-V representations are possible, the general qualitative features and trends are expected to remain well represented by this current approach.

In order to study the failure of GB barrier dominated ZnO samples, simulations were carried out with a bias chosen to make the current density equal to 100A/cm^2. Two different disorder parameters d=1 and d=5 were used in a Voronoi network with 492 grains. For each disorder parameter, the average grain size was varied from 1 μm to 30 μm. For grains reaching this melting threshold, the I-V characteristics were switched to those of (7) in a dynamic fashion. Thus, this procedure allowed the sequential analysis of successive localized failures and phase-transitions. Our time-dependent simulations were continued in time without any dynamic I-V updates as long as the grains remained below 820˚C and the 137.9 MPa critical stress threshold [13] was not reached.

III. RESULTS AND DISCUSSION

Figure 3 shows the global voltage for d=1 and d=5 necessary to drive a sample current density of 100 A/cm^2. A Voronoi network with 492 grains and a Gaussian distribution of barrier voltages V_B was used. As evident from Fig. 3, the bias voltage is predicted to increase, as the disorder parameter gets smaller. A higher disorder

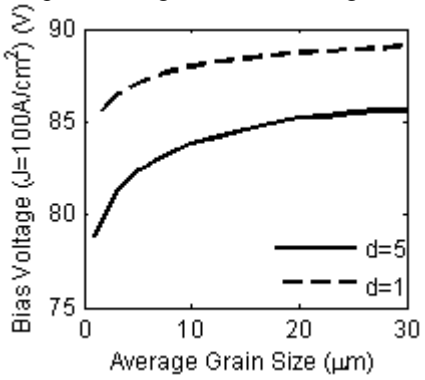

Figure 3. Variation of bias voltage with different grain sizes for a current density J = 100 A/cm^2.

parameter "d" implies a more heterogeneous granular structure with higher variability. A sample under such conditions, tends to have many grains that are larger than average. If a collection of such larger grains happens to lie within a random anode-to-cathode path, then the number of grain boundaries encountered between the electrodes would correspondingly be lower. Since the sample resistance mainly comes from grain boundary contributions, such a random path between the electrodes would present the weakest resistance to current flow, and allow for highest Joule heating. Thus, the presence of

such heterogeneous grains provides a larger probability for current channeling via a low resistance path. The net result would be a decrease in the requisite bias voltage as predicted here in our simulations.

Next, time-dependent simulations were carried out starting with the bias voltages of Fig. 3 until the maximum temperature of the samples reached the 1093˚K melting point. Figures 4 and 5 show the global average temperature and maximum thermal stress for different grain sizes, respectively. These plots are snapshots obtained at instants that the melting points were reached. In Figures 4 and 5, the smaller the grain size, the higher is the global average temperature and smaller the maximum thermal stress. Also, the lower disorder parameter (d=1),

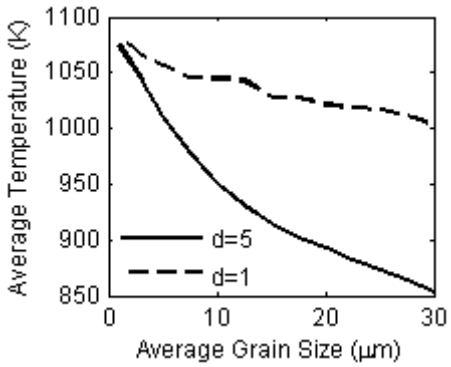

Figure 4. Variation of global average temperature with grain size when the maximum temperature is 1093˚K.

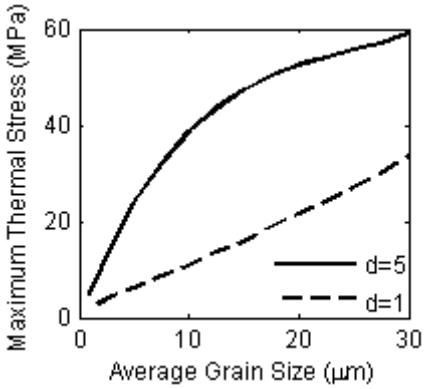

Figure 5. Variation of maximum thermal stress with ZnO average grain size when the maximum temperautre is 1093˚K.

yields a higher global average temperature and smaller maximum thermal stress. Furthermore, the smaller the grain size, the lower is the difference in average temperature and maximum thermal stress between the d=1 and d=5 cases. For example, for the 1 μm average grain size, the differences in temperature and stress were as small as 9.2 K and 3.04 MPa, respectively, between the d=1 and d=5 configurations. Very simply, these results imply that if the average grain size can be made sufficiently small, then individual variances in grains will have a minimal affect on the thermal characteristics of ZnO varistors. In addition, the maximal thermal stress is predicted to be the lowest for smaller grains, indicating an optimal strategy for practical varistor design.

Figure 6 shows the variation in bias duration until localized melting for different grain sizes and disorder parameters. The bias duration for d=1 is predicted to be longer than that for d=5, with the difference becoming

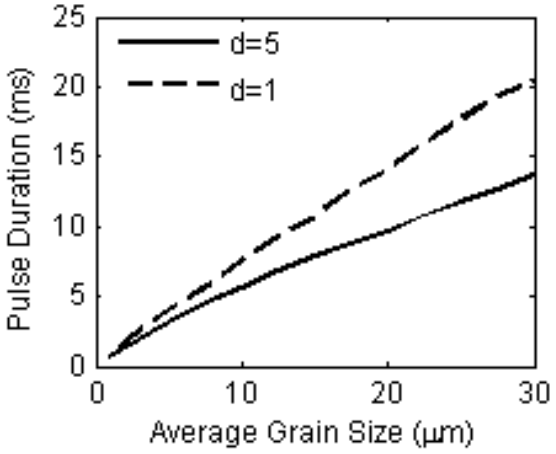

Figure 6. Relationship between bias durations and grain sizes corresponding to the maximum 1093˚K internal threshold.

smaller as the grain size reduces from 30 μm to 1 μm. With smaller average grains, the average internal temperatures generated are larger. Consequently, the external bias can only be applied up to a shorter duration before internal melting and sample damage. Hence, while reductions in grain size have the advantage of higher hold-off fields and more compact structures, this occurs at the expense of shorter external voltage durations. Alternatively, better thermal management and heat dissipation systems would be needed for the more compact varistors.

Table 2. The relative changes of properties when grain size changes from 30 μm to 1 μm.

Properties	**d = 1**	**d = 5**
Grain size	–96.7%	–96.7%
ZnO Sample volume	–99.996%	–99.996%
Bias voltage (J=100A/cm^2)	–4.4%	–7.9%
Average electric field	2767%	2663%
Average temperature	+8%	+26%
Maximum thermal stress	–94.6%	–91.7%
Average energy density	+20.4%	+31.9%
Bias duration	–95.6%	–95.1%

Table 2 lists the relative changes of electrical properties of the micro-structured ZnO varistiors with changes in the average grain size from 30 μm to 1 μm. The benefits of down-scaling the internal granularity is obvious. Stromg reductions in maximum thermal stress and sample size are predicted with negligible changes in hold-off voltage and average temperature. The average energy density is predicted to increase by about 20%, with a very large

increase in average electric field. The table indicates that greater uniformity within small grained samples should be preferred.

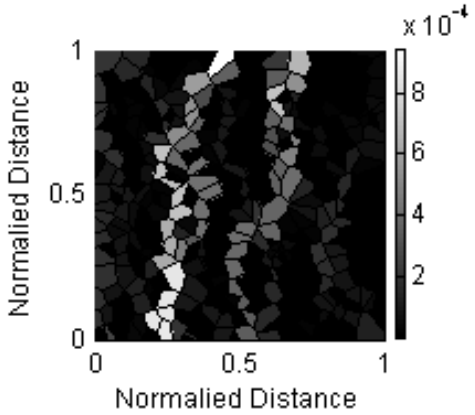

Figure 7. Snapshot of the internal current magnitude distribution for d=5 and an average grain size of 10 μm. Vertical scale denotes current in Amperes.

Next, the internal current distributions and temperature profiles are shown in Figs. 7 and 8. The former is a 5.8 ms snapshot of the internal maximum current magnitude distribution. The highest density in Fig. 7 is roughly at the lower left side, around the (0.2, 0.05) region. This also corresponds to the localized melting zone with maximum temperature of 1093˚K as predicted in Fig. 8.

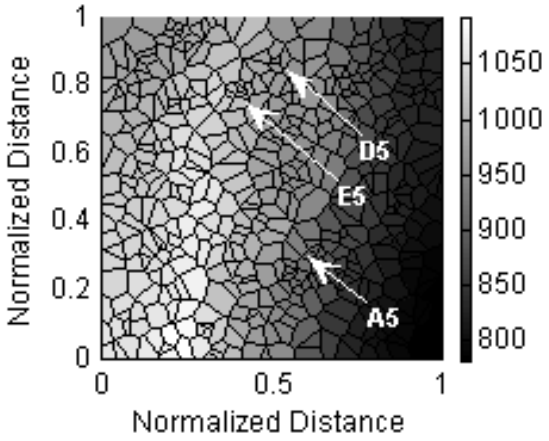

Figure 8. Snapshot of the temperature distribution for a 10 μm average grain size and d=5 sample. Vertical scale denotes temperature in Kelvin. Some specific locations are marked.

Fig. 9 shows the snapshot of GB melting and its temporal sequence for a d=5 sample. A progression of hot spots and the affected grain boundaries is evident in Fig. 10. The sequence of internally melted GBs is numbered and can be seen moving on either side of an initial "seed GB". For clarity, the cluster of GBs in the bottom-right region of Fig. 9 has been enlarged to better show the sequence numbering. For concreteness, the internal temperature evolution at four specific locations within the sample (as indicated in Fig. 8) is shown in Fig. 10. The non-uniformity in heating is obvious. The lowest temperature at ~5.8 ms is about 875˚K, while the highest is at the 1093˚K melting point. The maximum stress (not shown) was predicted to be about 39 Mpa. This is much less than the 137.9 MPa critical threshold needed for material cracking.

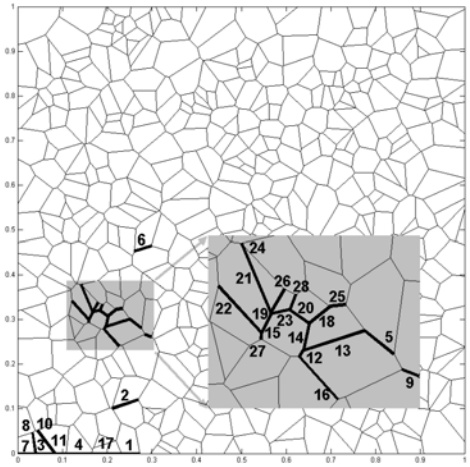

Figure 9. A 5.8 ms snapshot showing the grain boundaries in the granular ZnO sample with d=5. The numbers denote the melting sequence and the bottom-left shaded portion has been enlarged to reveal the numbers.

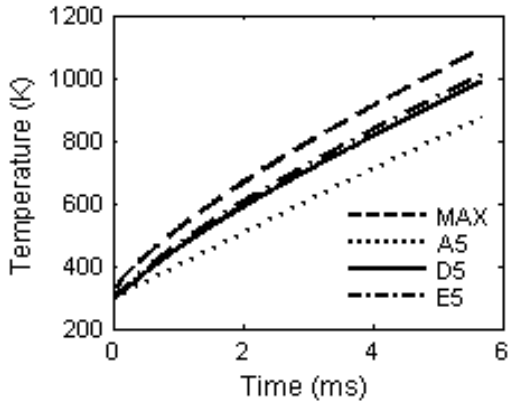

Figure 10. Time dependent temperatures at locations shown in Fig. 13 for d=5 and 10 μm average grain size. The simulation was terminated when the maximum temperature reached 1093˚K.

For completeness the above calculations of the time-dependent internal temperatures and thermal stresses were repeated for a lower (d=1) disorder parameter. The sequence of internal GB melting for the d=1 case is shown in Fig. 11. Since the non-uniformity in current distributions for this d=1 case is less pronounced than for the d=5 situation, there are fewer regions with large temperature differentials. Hence, instead of a few localized regions of very high temperature and melted GBs, a more gradual and smoother heating pattern results.

Thus, the number of "melted GBs" seen in Fig. 11 is higher and relative more spread out than in Fig. 9.

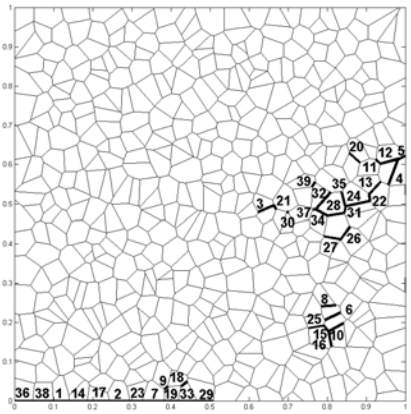

Figure 11. Snapshot showing grain boundaries in a d=1, ZnO sample. The numbers denote melting sequence.

IV. CONCLUDING SUMMARY

Time-dependent, two-dimensional simulations based on random Voronoi networks have been developed to study the internal heating and related breakdown effects in ZnO varistors in response to high-voltage pulsing.

Our results show that application of high voltage pulsing can lead to internal ZnO melting. Comparisons between relatively homogeneous (d=1) and more random (d=5) granular distributions were carried out. Our results predict that parameters such as the device hold-off voltage, the average internal temperature, and average dissipated energy density would be higher with more uniform grains. The d=1 case was also predicted to produce lower thermal stresses and to allow for the application of longer duration pulses. Furthermore, it was shown that scaling down the grain size offered advantages of increasing the device voltage hold-off, dramatic reductions in internal stresses and longer pulses.

Finally, it was shown that the principle failure mechanism would arise from internal localized melting and the transformation of GB characteristics associated with the phase transitions.

ACKNOWLEDGMENTS

This work was sponsored in part by a grant from Sandia National Laboratories (SNL).

REFERENCES

[1] L. M. Levinson and H. R. Philipp, "Zinc oxide varistors," *Am. Ceram. Soc. Bull.*, vol. 65, pp. 639-646, 1986.

[2] T. K. Gupta, "Application of Zinc Oxide varistors," *J. Am. Ceram. Soc*., vol.73, pp. 1817-1840, 1990.

[3] H. R. Philipp and L. M. Levinson, "Watts Loss and Conductivity Processes in ZnO Varistors", in Ceramic Transactions, Vol. 3: Advances in Varistor Technology, edited by L. M. Levinson (The American Ceramic Society, Westerville, OH, 1989), pp. 155-168.

[4] S. Boggs, J. Kuang, H. Andoh and S. Nishiwaki, "Electro-Thermal-Mechanical computations in ZnO arrester elements," *IEEE Trans. Power Delivery*, vol. 15, pp. 128-134, 2000.

[5] M. Bartkowiak, G. D. Mahan, and F. A. Modine, "Voronoi model of ZnO varistors with different grain boundaries," *J. Appl. Phys*., vol. 80, pp. 6516-6522, 1996.

[6] M. Tao, B. Ai, O. Dorlanne, and A. Loubiere, "Different ``single grain junctions" within a ZnO varistor," *J. Appl. Phys.*, vol. 61, pp. 1562-1567, 1987.

[7] H. Wang, W. Li, and J. Cordaro, "Single junctions in ZnO varistors studied by current-voltage characteristics and deep level transient spectroscopy" *Jap. J. Appl. Phys*., vol. 34, pp. 1765-1771, 1995.

[8] H. T. Sun, L. Y. Zhang, and X. Yao, "Electrical nonuniformity of grain boundaries within ZnO varistors," *J. Am. Ceram. Soc.*, Vol. 76, pp. 1150-1155, 1993.

[9] G. Zhao, R. P. Joshi, V. K. Lakdawala, and H. P. Hjalmarson, **"**Electro-Thermal Simulation Studies for Pulsed Voltage Induced Energy Absorption and Potential Failure in Microstructured ZnO Varistors," *IEEE Trans. Dielectr. Electr. Insul.*, in press.

[10] D. Weaire and N. Rivier, "Soap, cells and statistics – random patterns in two-dimensions," *Contemp. Phys.*, vol. 25, pp. 59-99, 1984.

[11] Q. Chen, J. He, K. Tan, et al, "Influence of grain size on temperature and thermal stress in ZnO varistor ceramics," *Science in China – Series E*, vol. 45, pp. 337-347, 2002.

[12] Y. S. Touloukian, R. W. Powell, C. Y. Ho, and P. G. Klemens, "*Thermophysical Properties of Matter*", IFI/Plenum, New York, vol. 2, pp. 243-245, 1970.

[13] M. Bartkowiak, M. G. Comber, G. D. Mahan, "Failure modes and energy absorption capability of ZnO varistors," *IEEE Trans. Power Delivery,* vol. 14, pp. 152-162, 1999.